The Effect of Varying Engine Conditions on Unregulated VOC-IVOC Diesel Exhaust Emissions

Kelly L Pereira[1], Rachel Dunmore[1], James Whitehead[2], M. Rami Alfarra[2,3], James D. Allan[2,3], Mohammed S. Alam[4], Roy M. Harrison[4,5], Gordon. McFiggans[2], Jacqueline F. Hamilton[1].

[1]Wolfson Atmospheric Chemistry Laboratories, Department of Chemistry, University of York, York, YO10 5DD, UK
[2]School of Earth, Atmospheric and Environmental Sciences, University of Manchester M13 9PL, UK
[3]National Centre for Atmospheric Science, UK
[4]School of Geography, Earth and Environmental Sciences, University of Birmingham B15 2TT, UK
[5]Department of Environmental Sciences / Center of Excellence in Environmental Studies, King Abdulaziz University, PO Box 80203, Jeddah, 21589, Saudi Arabia

Correspondence to: Jacqueline Hamilton (jacqui.hamilton@york.ac.uk)

Abstract

An extensive set of measurements were performed to investigate the effect of different engine conditions (*i.e*. load, speed, temperature, 'driving scenarios') and emission control devices (with/without diesel oxidative catalyst, DOC) on the composition and abundance of unregulated exhaust gas emissions from a light-duty diesel engine. Exhaust emissions were introduced into an atmospheric chamber and measured using thermal desorption comprehensive two-dimensional gas chromatography coupled to a flame ionisation detector (TD-GC×GC-FID). In total, 16 individual and 8 groups of compounds were measured in the exhaust gas, ranging from volatile to intermediate volatility. The total speciated VOC-IVOC (∑SpVOC) emission rates varied significantly with different engine conditions, ranging from 70 to 9268 milligrams of VOC mass per kilogram of fuel burnt (mg kg^{-1}). ∑SpVOC emission rates generally decreased with increasing engine load and temperature, and to a lesser degree, engine speed. The exhaust gas composition changed as a result of two main influencing factors, the DOC hydrocarbon (HC) removal efficiency and engine combustion efficiency. Increased DOC HC removal efficiency and engine combustion efficiency resulted in a greater percentage contribution of the C_7 to C_{12} branched aliphatics and C_7 to C_{12} *n*-alkanes, respectively, to the ∑SpVOC emission rate. At low engine temperatures (< 150°C), the contribution of *n*-alkanes in the exhaust gas increased with increasing combustion efficiency and may be important in urban environments, as *n*-alkanes are more efficient at producing SOA than their branched counterparts. At very high engine temperatures, the *n*-alkane contribution increased by a factor of 1.6 times greater than observed in the cold-start experiment (most similar to unburnt fuel) and may suggest liquid fuel based estimates of secondary organic aerosol (SOA) yields may be inconsistent with exhaust SOA yields, particularly at high engine temperatures (*i.e.* high engine speeds and loads). The investigated DOC removed 46 ± 10 % of the ∑SpVOC emissions, with removal efficiencies of 83 ± 3 % for the single-ring aromatics and 39 ± 12 % for the aliphatics (branched and straight-chain). The DOC aliphatic removal efficiency generally decreased with increasing carbon chain length.

To our knowledge, this is the first study which has explicitly discussed the effect of the DOC HC removal efficiency and combustion efficiency on the exhaust gas composition. With further work, compositional differences in exhaust gas emissions as a function of engine temperature, could be implemented into air-quality models, resulting in improved refinement and better understanding of diesel exhaust emissions on local air quality.

1. Introduction

Urban air pollution is detrimental to human health, adversely effecting air quality and resulting in increased morbidity and mortality rates (Han and Naeher, 2006; Cohen et al., 2005; Prüss-Üstün and Corvalán, 2006). The World Health Organisation attributed 1.34 million premature deaths to urban air pollution in 2008 (WHO, 2006; Krzyzanowski and Cohen, 2008). Of these deaths, 1.09 million could have been prevented if the air quality guidelines had been met (WHO, 2006; Krzyzanowski and Cohen, 2008). Over half of the world's population now live in urban areas (Prüss-Üstün and Corvalán, 2006; UnitedNations, 2014). By 2050, this populous is expected to grow to 6.34 billion people, with an estimated 66% of the world's population living in urban environments (Prüss-Üstün and Corvalán, 2006; UnitedNations, 2014). Road transport emissions are a dominant source of urban air pollution (DEFA, 1993; Colvile et al., 2001; HEI, 2010) with common road-traffic pollutants including gaseous hydrocarbons (including volatile organic compounds, VOCs), nitrogen oxides (sum of NO + NO_2), carbon oxides (CO and CO_2) and particulate matter (PM), with secondary reaction processes resulting in the formation of ozone and secondary aerosol (WHO, 2006; HEI, 2010). Exposure to road-traffic air pollutants, both primary and secondary, are of a major health concern (UnitedNations, 2014; WHO, 2006; HEI, 2010). Secondary aerosol formation from diesel and gasoline powered motor vehicles has received considerable attention in recent years (Gentner et al., 2017). There is currently considerable debate as to whether diesel or gasoline powered motor vehicles are more important for secondary organic aerosol (SOA) formation and which precursors are the most efficient at forming SOA (Gentner et al., 2017). In Europe, almost half of all new passenger cars are diesel (49.5%), with petrol (45.8%), electric hybrids (2.1%), electric (1.5%) and alternative fuels (1.2%) accounting for the remaining fraction (ACEA, 2016). Diesel exhaust emissions vary considerably with vehicle type, age, operation conditions, fuel, lubricant oil and emission control devices, among other factors (HEI, 2010). Emission regulations of nitrogen oxides, carbon monoxide, PM and total hydrocarbon mass has resulted in the reduction of exhaust emissions (HEI, 2010). However, this 'blanket approach' for the reduction of total hydrocarbon mass, has in-part, resulted in few studies investigating the detailed chemical composition of exhaust emissions with varying engine conditions (Yamada et al., 2011). Another contributing factor, is the difficulty in exhaust gas measurement (Yamada et al., 2011; Rashid et al., 2013). On-road measurements of exhaust gas are difficult, due to the continually evolving chemical composition, requiring techniques capable of providing detailed chemical speciation in real-time, or near-real-time. Furthermore, the abundance of gaseous compounds in exhaust emissions often involves lengthy quantification processes. The detailed chemical characterisation of exhaust gas with varying engine conditions however, can considerably aid emission inventories and provide a greater understanding of

exhaust emissions on local air quality. In addition, this information could serve to influence the design of emission control devices, reducing the emission rates of potentially harmful unregulated exhaust gas components.

On-road measurements of unregulated exhaust gas emissions are often performed in tunnels, on roadsides, or motorways (*e.g.* (Gentner et al., 2013; Liu et al., 2015; Ježek et al., 2015; Zavala et al., 2006; Jiang et al., 2005; Kristensson et al., 2004; Fraser et al., 1998; Miguel et al., 1998; Staehelin et al., 1998)). These measurements provide a compositional overview of the exhaust emissions from the on-road vehicular fleet, consisting of a vast range of vehicle types (*e.g.* light-duty, heavy-duty), emission control devices (*e.g.* with/without exhaust gas recirculation) and fuel composition (*e.g.* ultra-low sulfur diesel (ULSD), super unleaded petrol, premium unleaded petrol, biofuel, among others). These measurements however, do not allow the effect of different engine conditions or emission control devices on the exhaust gas composition to be investigated. Dynamometer engines or chassis dynamometers can afford compositional insight into exhaust emissions with varying engine conditions, providing a high degree of control and reproducibility (Tadano et al., 2014; Louis et al., 2016). Several studies have used dynamometers to investigate the changes in unregulated exhaust gas composition with the use of different transient driving cycles, for petrol engines (Pang et al., 2014; Baldauf et al., 2005), diesel (Yamada et al., 2011; Cross et al., 2015; Schauer et al., 1999; Zhao et al., 2015; Ballesteros et al., 2014; Nelson et al., 2008; Siegl et al., 1999; Westerholm et al., 1991), or both (Alves et al., 2015; Chirico et al., 2014; Alkurdi et al., 2013; Caplain et al., 2006; Schmitz et al., 2000; Louis et al., 2016). Driving cycles (often performed with a chassis dynamometers) are designed to simulate real-world driving conditions, allowing the exhaust emissions from individual vehicles to be investigated. However, these driving cycles offer limited information on the effect of combustion or specific engine conditions (*e.g.* engine load, speed) on unregulated exhaust emissions, due to the averaging of emissions over entire driving cycles and lack of steady-state engine conditions (Cross et al., 2015); compositional information which is easily obtained with the use of a single-engine dynamometer rig ((Chin et al., 2012; Cross et al., 2015; Zhu et al., 2013; Schulz et al., 1999; Machado Corrêa and Arbilla, 2008)). Recent studies have focused on the measurement of intermediate-VOCs in diesel exhaust emissions, primarily due to advances in instrumentation to allow the detection of these species. IVOCs have an effective saturation concentration (C^*) of 10^3 to 10^6 µg m^{-3} and reside almost exclusively in the gas-phase at atmospheric conditions (Donahue et al., 2006). IVOCs comprise a considerable fraction of diesel exhaust emissions, with studies attributing ~ 20 to 60% of the non-methane organic gases to IVOCs (Schauer et al., 1999; Siegl et al., 1999; Zhao et al., 2015; Gordon et al., 2014). IVOC diesel exhaust emissions are relatively poorly characterised, yet are contribute significantly to SOA formation (Gentner et al., 2017). Recently, Cross et. al (2015) investigated IVOC diesel exhaust emissions using a dynamometer rig. It was found that IVOC diesel exhaust emissions were highly dependent on engine power. At low engine loads, the exhaust gas composition was dominated by saturated hydrocarbons, likely the result of unburnt fuel. At high engine loads however, the exhaust gas composition changed, including newly formed unsaturated hydrocarbons and oxidised compounds from incomplete combustion (Cross et al., 2015). Furthermore, Chin et. al. (2012) found the composition of VOC and IVOC diesel exhaust emissions (generated under steady-state engine conditions) depended on engine load, fuel type (ULSD and biodiesel) and emission control devices.

This study investigates the compositional changes of unregulated exhaust emissions with varying engine conditions (*i.e.* engine load, speed and 'different driving scenarios') and emission control devices (with/without DOC) using a dynamometer rig. In contrast to previous studies, , this work combines both detailed chemical speciation and groupings of VOC – IVOCs (C^* 10^5 to 10^8 μg m^{-3}) based on their structure and functionality, providing a more detailed compositional overview of the effect of different engine conditions on exhaust gas emissions. In addition, to our knowledge, this is the first study which attempts to decouple the effect of the diesel oxidation catalyst (DOC) and combustion efficiency on the exhaust gas composition. The emissions from a light-duty 1.9L Volkswagen diesel engine were investigated. Exhaust emissions from different engine conditions were introduced into an atmospheric chamber which was used as a 'holding-cell' for sampling, allowing lower time resolution techniques to be used. In total, 16 individual and 8 groups of compounds were measured in the exhaust gas using comprehensive two-dimensional gas chromatography coupled to a flame ionisation detector (GC×GC-FID). The effect of different engine conditions and emission control devices on the composition and abundance of the speciated VOC-IVOCs is discussed. Finally, the possible atmospheric implications of these results are discussed.

2. Experimental

2.1 Chamber setup

Experiments were performed in the Manchester Aerosol Chamber (MAC) located within the University of Manchester, UK. The MAC consists of an 18 m^3 fluorinated ethylene propylene (FEP) Teflon bag with the following dimensions; 3m (L) × 3m (W) × 2m (H). The chamber is supported by three rectangular aluminium frames, two of which are free moving, allowing the chamber to expand and collapse as sample air flow is introduced or extracted. Irradiation is achieved through a series of wall mounted halogen lamps (Solux 12V, 50W, 4700K, New York, USA) and two filtered 6 kW Xenon Arc lamps (XBO600W/HSLA OFR, Osram, Germany) located within the chamber enclosure. Purified air is used within the chamber and is humidified prior to introduction. A suite of instruments was used to measure chamber temperature (series of cross-calibrated thermocouples), relative humidity (Dewmaster chilled mirror hygrometer, Edgetech Instruments, USA), CO_2 (model 6262, Li-Cor Biosciences, USA), NO_x (model 42i, Thermo Scientific, MA, USA), O_3, (model 49C, Thermo Scientific, MA, USA) and VOC-IVOCs (comprehensive two-dimensional gas chromatography flame ionisation detection, see below for further details). Particle number, mass and diameter were measured using a differential mobility particle sizer (DMPS (Williams et al., 2007)) consisting of a differential mobility analyser (DMA (Winklmayr et al., 1991)) and a condensation particle counter (CPC, model 3010, TSI Inc., USA). Further technical information regarding the chamber design can be found in Alfarra et al. (2012).

2.2 Engine and exhaust sampling system

The emissions from a light-duty Volkswagen (VW) 1.9L diesel engine was investigated. A schematic of the dynamometer and exhaust sampling system is shown in SI Figure S1. The engine had 4 cylinders with a capacity of 1896 cm^3 and a compression ratio of 19.5 : 1. The engine was mounted on an eddy current dynamometer rig (CM12, Armfield Ltd, Hampshire, UK) and

the exhaust connected to a new (0 mileage hours) retrofitted DOC. The DOC was purchased from a local garage (Oldham Tyre and Exhaust, Oldham, UK) and consisted of a mix of platinum and rhodium. No diesel particulate filter (DPF) was used, conforming to Euro 4 emission control regulations. The auto-equivalent version of this engine has been used in several VW polo and Jetta models in the early 2000's and was chosen as an example of light-duty diesel engine. The aftertreatment was selected to meet Euro 4 emission control regulations required for such models. Engine running parameters (*i.e.* rpm, load, and throttle) were controlled using a dedicated software package (Armfield Ltd, Hampshire, UK) on a separate PC. The engine temperature was measured *via* an in-built thermocouple located inside the engine exhaust pipe, next to the engine. The DOC temperature has been inferred from the measured exhaust temperature. The DOC temperature will be lower than the measured exhaust temperature, due to the DOC being located further down the exhaust pipe. A 2-meter-long, 2-inch bore, stainless steel tube with a computer controlled pneumatic valve, was used to allow the engine emissions to be introduced into the MAC or diverted to waste. The timed control of the pneumatic valve allowed a proportion of the exhaust emissions to be introduced into the chamber, controlling dilution. The final exhaust dilution ratios were calculated from the measured CO_2 concentration prior to, and after the introduction of the exhaust emissions. Further information regarding the exhaust dilution calculations can be found in Whitehead et al. (2017, in preparation). The engine was fuelled with standard European (EN590 specifications, Euro 5 compliant) ULSD obtained from a local fueling station. Two batches of fuel were obtained, the first in June 2014 (batch A) and the second in November 2014 (batch B). A second batch of fuel was required due to a considerable increase in the number of planned experiments. The fuel batches were of the same specification and obtained from the same local fueling station. Batch A was used in experiments 1 to 9 and batch B in experiments 10 to 16 (see Table 1 and section 3.1.1). The sulphur content was < 10 ppm. Further information regarding the standard European ULSD fuel specifications can be found in 2009 EC directive (EU, 2009).

2.3 Experimental design

A series of experiments were performed in July to August 2014, November 2014, and September to October 2015, as a part of the project, COMbustion PARTicles in the atmosphere (Com-Part). Experiments were designed to systematically characterise the chemical and physical transformations of primary and secondary particles emitted from a light-duty diesel engine under a range of atmospheric dilution and oxidation conditions. The work characterised the transformation of gaseous and particulate phase emissions across a range of steady-state engine conditions. The results shown here, focus on the effect of different engine conditions on the composition and abundance of VOC-IVOCs in the raw exhaust emissions, which formed a subset of the total number of experiments performed. The experimental descriptions and engine operating parameters discussed here, can be found in Table 1. A range of engine conditions were studied, including: (i) engine speed, ranging from 1150 rpm (idle) to 3000 rpm (maximum engine output), (ii) engine load, ranging from 0 % (no load) to 53 % (the maximum load which could be safely applied to by the dynamometer in the experimental setup), (iii) emission control devices (with and without the DOC) and, (iv) 'driving scenarios' (see below for further details). The MAC was filled with clean air prior to the introduction of the exhaust emissions. Exhaust dilution ratios were varied to represent a range of ambient conditions from near to downwind of an emission

source, capturing the chemical and physical transformations of semi-volatiles in the exhaust emissions with varying ambient dilutions.

The majority of experiments focused on steady-state engine conditions, where selected engine running parameters were applied to the engine and the engine temperature allowed to stabilise, prior to the introduction of the exhaust emissions into the MAC. Steady-state engine conditions are defined here, as a constant engine temperature within ±10% of the steady-state average. Steady-state engine conditions were not performed for the 'driving scenario' (exp. 8 and 9, see Table 1) and cold-start experiments (exp. 6, 7 and 14, Table 1), with the cold-start experiments requiring exhaust injection into the MAC after ~ 1 to 2 minutes of engine start-up (*i.e.* cold-engine). A sequence of engine conditions was performed for the driving scenario experiments, with the injection of the exhaust emissions into the MAC after the completion of the sequence, but prior to achieving steady-state engine conditions. These experiments were performed to gain a greater insight into engine conditions controlling VOC-IVOC emission rates. The sequence of engine conditions used in the driving scenario experiments, 'cold loaded' (exp. 8, Table 1) and 'warm idle following load' (exp. 9, Table 1) are shown in Table 1, and SI Figure S2. All experiments except experiment 3 (see Table 1) were performed with the DOC. This allowed the combined effect of the DOC and different engine conditions on the exhaust emissions to be observed; engine conditions most representative of on-road diesel vehicles.

2.4 TD-GC×GC-FID

VOC-IVOC exhaust emissions were measured using thermal desorption comprehensive two-dimensional gas chromatography with a flame ionisation detector (TD-GC×GC-FID) operating at 200 Hz. A TT24-7 thermal desorption unit (Markes International, Llantrisant, UK) with an air server attachment was used for sample collection. The inlet of the TD unit was connected to MAC using ~ 2.5 meters of heated 1/4" stainless steel tubing. The stainless steel tubing was heated to ~ 70 °C to reduce condensational losses of VOCs. An in-line unheated particulate filter prevented sampled particles from entering the TD unit. The in-line filter was replaced prior to each experiment, minimising particulate loadings. A clean air diaphragm pump (model PM25602-86, KNF Neuberger, Oxfordshire, UK) was used to extract an overflow of sample air from the MAC, a proportion of which was sampled into the TD unit. Two sequential glass traps cooled to -20 ˚C in an ethylene glycol bath were used to remove water vapour from the sampled air. No significant VOC losses have been found using this method of water vapour removal (Lidster, 2012). Air samples were trapped onto Tenax sorbent tubes (Markes International, Llantrisant, UK) held at -10˚C during sampling (26 minute sampling duration) and heated to 230˚C upon desorption.

An Agilent 7890 GC (Agilent Technologies, Wilmington, USA) with a modified modulation valve, consisting of a 6-port, 2-way diaphragm valve (Valco Instruments, Texas, USA) and 50 µL sample loop (Thames Resteck, UK) was used (see Lidster et al. (2011) for further information). Cryogenic cooling (liquid CO_2, BOC, UK) was used to re-focus the sample on the head of the primary column upon desorption. Compound separation was achieved using a primary 25 meter 5% phenyl

polysilphenylene-siloxane column (BPX5, SGE, Ringwood, Australia) with a 0.15 mm internal diameter and 0.4 µm film thickness, and a secondary 7-meter polyethylene glycol column (BP20 SGE, Ringwood, Australia) with a 0.25 mm internal diameter and 0.25 µm film thickness. Helium (CP grade, BOC, UK) was used as the carrier gas. Primary and secondary column pressures were controlled using an electronic pneumatic control (Agilent 7890 EPC) and were set at 50 and 23 psi, respectively. The modulator was heated to 120˚C with a 5 second cycle time, comprising of 0.3 second injection and a 4.7 second sample introduction. The oven temperature program consisted of a two-stage ramp; holding at 70˚C for 1 minute, increasing to 160˚C at 16 minutes (6˚C min^{-1}), then 200˚C at 20 minutes (10˚C min^{-1}) with an additional 2-minute hold, giving a total runtime of 22 minutes. The FID heater was set to 300˚C with a hydrogen flow of 30 ml min^{-1} (CP grade, BOC, UK) and an air flow of 300 ml min^{-1} (BTCA 178 grade, BOC UK). A National Physical Laboratory (NPL30, Teddington, UK) gas standard (see SI) was used to monitor instrument variability over the course of the experiments. VOC-IVOC concentrations were determined using either the NPL gas standard or the relative response factors (RRF) of liquid standards (see SI for further information). Calibrations were performed weekly using the NPL gas standard, or more frequently during instrument maintenance periods. The instrument detection limits for the investigated compounds can be found in the SI of Dunmore et al. (2015). Where possible, compounds were integrated using GC Image software (Zoex Corporation, Houston, USA). The abundance of VOC-IVOCs in the diesel exhaust emissions and the fast method runtime, resulted in some peaks having poor resolution. The automated peak integration in the GC Image software package was unable to distinguish closely eluting peaks, resulting in the use of one-dimensional chromatographic integration using Chemstation (Agilent, CA, USA). The minimum peak volume was set to 10 pixels for the automated peak integration in GC Image software. Only samples where no changes had been made to the chamber conditions were analysed. The exhaust emissions were blank subtracted using the chamber background measurement/s prior to the introduction of the exhaust emissions. In two experiments (exp. 1 and 6, see Table 1), the chamber background measurements were deemed unsuitable for the use of blank subtraction due to changing chamber conditions (*e.g.* cleaning cycle had not completed before blank sampling had started). Instead, the most recent chamber background measurement to that experiment was used. The GC×GC-FID started sampling during chamber cleaning and sampled for 26 minutes per analysis. The sampling start time was on average 13 minutes after exhaust injection (see SI Table S2). A minimum of two replicate measurements of the exhaust emissions was performed for the majority of experiments. The emission rates shown are averages of the replicate measurements. No apparent losses of the VOC-IVOCs were observed during sampling. The relative standard deviation from replicate measurements, of the investigated compounds over ~ 2 hours of sampling (longest sampling time period investigated), ranged between 1.9 to 14.2%, with an average of 6.4% (exp. 6, see Table 1 and SI Table S2.

2.5 Liquid fuel analysis

The two batches of ULSD fuel (see section 2.2 and 3.1.1) were analysed using comprehensive two-dimensional gas chromatography (model 6890N, Agilent Technologies, UK) coupled to a time-of-flight mass spectrometer (Pegasus 4D, Leco, MI, USA) (GC×GC-TOFMS). Compound separation was achieved using a primary 15 meter 5% phenyl polysilphenylene-

siloxane (BPX5, SGE, Ringwood, Australia), column with a 0.25 mm film thickness and 0.25 mm internal diameter, and a secondary 2 meter 50% phenyl polysilphenylene-siloxane (BPX50, SGE, Ringwood, Australia) column with a 0.25 mm film thickness and 0.25 mm internal diameter. Samples were introduced into the GC×GC-TOFMS using a Gerstel multipurpose sampler (MPS 2, Gerstel, USA) with dedicated controller (model C506, Gerstel, USA). A 1 µL injection volume was used with a split ratio of 100:1. The transfer line was set to 270°C. Cryo-jet modulation cooling was used to achieve comprehensive two-dimensional separation. Helium (CP grade, BOC, UK) was used as the carrier gas with a constant flow rate of 1.5 ml min^{-1}. The oven starting temperature was set to 65°C with a 0.2 minute hold, followed by a temperature ramp of 4°C min^{-1} to 240°C, with a further 10 minute hold. The modulator and secondary oven temperature was set to 15°C and 20°C above the oven temperature, respectively. The TOFMS acquisition rate was set to 50 spectra per second, with a scan range of mass-to-charge (*m/z*) 35 to 500. The data was analysed using Leco ChromaTOF software version 4.51.6 (Leco, MI, USA). Compounds were identified using the National Institute of Standard and Technology (NIST) standard reference database (version 11).

3. Results and discussion

A series of experiments were performed as a part of the project, COMbustion PARTicles in the atmosphere (Com-Part), investigating the effect of different engine conditions (*i.e.* speed, load, 'driving scenarios'), exhaust dilution ratios and emission control devices (with and without the DOC) on the composition and abundance of VOC-IVOCs in the exhaust emissions from a light duty VW diesel engine. The experimental dates, descriptions and engine operating parameters are shown in Table 1. This study focuses on steady-state engine conditions, allowing the direct comparison of engine speed and load on VOC-IVOC emission rates, which would otherwise not be captured with the use of transient driving cycles. A variety of engine loads and speeds were investigated, ranging from 0 (no load) to 53% load (maximum load which could be safely applied by the dynamometer in the experimental setup) and a speed of 1150 (idling) to 3000 rpm (maximum engine output). Further details regarding the experimental design can be found in section 2.3. A proportion of the exhaust emissions from each experiment (see Table 1) were introduced into the MAC. The MAC was used as a holding-cell, allowing multiple instruments and instruments requiring longer sampling times than near-real time to be used.

VOC-IVOC emissions were measured using TD-GC×GC-FID. In total, 16 individual and 8 groups of compounds were speciated. The individual compounds included nine single-ring aromatics: benzene, toluene, ethyl benzene, meta- and para-xylene (grouped), ortho-xylene, styrene, 1,3,5-TMB, 1,2,4-TMB and 1,2,3-TMB, and 7 *n*-alkanes from *n*-heptane to *n*-tridecane. Grouped compounds consisted of C_7 to C_{13} branched aliphatics grouped by carbon number and single-ring aromatics with three carbon substitutions (*i.e.* those in addition to the trimethylbenzene isomers above). The emission rates of *n*-tridecane and the C_{13} branched aliphatic grouping were not measured in some experiments due to a shift in the instrument retention time, resulting in these species not being observed. The saturation concentration (C^*, µg m^{-3} (Donahue et al., 2006)) of the speciated compounds ranged between 10^5 –10^8 µg m^{-3}, classifying these species as intermediate to volatile organic compounds (VOC-

IVOCs). The most abundant volatility fraction of IVOCs from diesel exhaust emissions were measured, see Zhao et al. (2015) for further information. An annotated chromatogram displaying the speciated compounds, is shown in Figure 1. The use of two different stationary phases in GC×GC allows compounds to be separated by two physical properties, such as boiling point and polarity, as shown here (see Figure 1). This two-dimensional separation, creates a characteristic space where compounds are grouped by similar physical properties (*e.g.* aromatic and aliphatic bandings (see Figure 1, *c.f.* Hamilton and Lewis (2003), Dunmore et al. (2015)), aiding in the identification of unknowns. This characteristic space, in combination with the use of commercially available standards and the elution patterns observed in previous work using this instrument (Dunmore et al., 2015), allowed 8 compound groupings to be identified. The identification of all the individual compounds (except styrene, see SI) were confirmed using commercially available standards. The emission rates of the individual and grouped compounds and their percentage contribution to the total speciated VOC-IVOC emission rate (hereafter referred to as ∑SpVOC), are shown in the SI Tables S3 to S6. No corrections have been made for gas-phase absorption to PM in this work. Gas-phase absorption to PM is negligible due to the relatively high vapour pressures of the compounds speciated, low VOC-IVOC mixing ratios and small amount of aerosol mass present after exhaust dilution.

3.1 Experimental reproducibility

The reproducibility of the measured VOC-IVOC emission rates with different engine conditions and exhaust dilution ratios were investigated and are discussed below. The emission rates from two replicate cold-start experiments (1150 rpm, 0% load, exp. 6 and 7, see Table 1) and two replicate warm with load (WWL) experiments (2000 rpm, 30% load, exp. 15 and 16, see Table 1) are shown in Figure 2 and SI Figure S3, respectively. Both replicate experiments were performed with similar exhaust dilution ratios. The emission rates from the replicate cold-start and WWL experiments displayed excellent reproducibility, considering the vast number of variables in these experiments (*e.g.* combustion and DOC HC removal efficiency). All emission rates, except styrene in one experiment (< limit of detection), were observed to be within the calculated uncertainty (see SI). The emission rates from two replicate warm high load experiments (2500 rpm, 40% load, exp. 1 and 2, see Table 1) with different exhaust dilution ratios is shown in SI Figure S4. The exhaust dilution ratios in these experiments were 166 and 313 in experiments 1 and 2 (see Table 1), respectively. The emission rates in these experiments are relatively comparable. Only one measurement of the exhaust emissions was made in each experiment. The majority of experiments had a minimum of two replicate measurements of the exhaust emissions (see SI Table S1), possibly accounting for slight differences observed in the measured VOC-IVOC emissions rates.

The emission rates from two replicate WWL experiments (2000 rpm, 30% load, exp. 4 and 5, see Table 1) at the extremes of the investigated exhaust dilution ratios are shown in SI Figure S5. The exhaust dilution ratios were 1158 and 60 in experiments 4 and 5, respectively. The emission rates in these experiments displayed some disagreement. The engine thermocouple was unresponsive during one of these experiments (exp. 4, see Table 1). Consequently, it is not known if steady-state engine conditions were achieved prior to the introduction of the exhaust emissions into the MAC and whether the engine temperature

upon injection was comparable to replicate experiment, possibly accounting of the observed differences in the VOC-IVOC emission rates. Nevertheless, no experiments with such large differences in the exhaust dilution ratios have been directly compared in the following work and where engine conditions are compared, experiments with similar exhaust dilution ratios and engine temperatures have been used. These experiments highlight the importance of replicate measurements and the comparison of VOC-IVOC emission rates from experiments with similar engine temperatures. A propagation of errors was calculated to determine the uncertainty in the measured emission rates and is discussed in the SI. The uncertainty in the measured emission rates for the investigated compounds, ranged from 6 to 50 %, with an average of 22%.

3.1.1 ULSD fuel: Batch A and B

Two batches of ULSD fuel were used (see section 2.2). Both batches of fuel were of the same specification and obtained from the same local fueling station. One batch was purchased in June 2014 (batch A, used in experiments 1 to 9) and the second, in November 2014 (batch B, used in experiments 10 to 16). The emission rates from three replicate cold-start experiments, two using fuel batch A (exp. 6 and 7, see Table 1) and one using fuel batch B (exp. 14), are shown in Figure 3. From Figure 3, it can be observed that there is a considerable difference in the emission rates of the C_7 to C_{12} branched aliphatics between replicate experiments 6 and 7, and experiment 14. The emission rates of the C_7 to C_{12} branched aliphatics decreased by a factor of ~ 4 with the use of fuel batch B (exp. 14). The excellent agreement of the emission rates between replicate cold-start experiments 6 and 7, suggests the compositional differences observed in experiment 14, is the result of a slight difference in the fuel composition between batches A and B. GC×GC-TOFMS was used to further investigate any compositional differences between the fuel batches. An extensive analysis of the diesel fuel was not performed. The aim of this analysis was to investigate whether there were any apparent differences in the fuel composition that would prevent a direct comparison of the emission rates from fuel batches A and B. An extracted ion chromatogram for *m/z* 57 (dominant aliphatic fragment ion) from fuel batch A and B is shown in SI Figure S6 A and B, respectively. The chromatograms were normalised to the total peak area to allow direct comparison of peak intensity between the chromatograms. The highlighted region in SI Figure S6 displays straight-chain and branched aliphatics with a carbon number range of approximately C_7 to C_{12} (determined from the NIST library). The peak intensities in the chromatograms from fuel batches A and B are largely comparable, except for the highlighted region, where a slightly lower peak intensity is observed in fuel batch B. As a result, the emission rates from fuel batches A and B have not been directly compared. The reason for the observed compositional differences between fuel batches A and B is unclear, although suggests a possible change in the refining process between the purchase of both fuel batches.

3.2 Engine load

The ∑SpVOC emissions were observed to decrease with increasing engine load, with ∑SpVOC emission rates of 1019±65, 365±24 and 70±4 mg kg^{-1} at 30, 40 and 53% load, respectively (see SI Table S7). This trend of decreasing VOC emission rates with increasing engine load has been observed in a number of previous studies for light-duty and medium-duty diesel vehicles (Cross et al., 2015; Shirneshan, 2013; Chin et al., 2012; Yamada et al., 2011) and can be explained by considering the engine

operation. At low engine temperatures (*i.e.* low engine loads and idling conditions), the fuel flow is increased to provide easily combustible conditions within the engine cylinder. This additional fuel flow creates a rich air/fuel ratio, where there is insufficient oxygen to burn the fuel, resulting in incomplete combustion and higher VOC-IVOC emission rates from the unburnt fuel. As the engine temperature increases (*e.g.* with increasing engine load), the in-cylinder oxidation rate increases as the fuel components become more easily combustible at higher temperatures, increasing combustion efficiency and decreasing VOC-IVOC emission rates (Heywood, 1988). The effect of different engine loads, at a constant speed, on the VOC-IVOC emission rates is shown in Figure 4A. The VOC-IVOC emission profiles are characteristic of typical diesel exhaust emissions with a DOC (*c.f.* (Chin et al., 2012; Bohac et al., 2006)), displaying a high abundance of C_8 to C_{12} *n*-alkanes and C_8 to C_{13} branched aliphatics, with a smaller contribution from single-ring aromatics. The carbon number distribution of the *n*-alkanes and branched aliphatics at 30% and 40% engine load are comparable. Branched aliphatics display an increase in abundance from C_7, reaching peak concentration at C_{10}, followed by a decrease to C_{13}, similar to that observed in Bohac et. al. (2006). Straight-chain alkanes do not display the same increase and decrease in abundance, with the emission rates of *n*-nonane and *n*-dodecane greater than *n*-undecane, displaying no obvious trend. At 53% engine load, the emission profile changes. The most abundant *n*-alkane and branched aliphatic grouping shifts to higher carbon numbers at higher loads, changing from *n*-nonane to *n*-undecane and from C_{10} to C_{12} branched aliphatics. The *n*-alkanes now display a sequential increase and decrease in their emission factors, as observed with the branched aliphatics. This compositional shift to higher carbon number species under higher engine loads, has also been observed in Chin et al. (2012) for *n*-alkanes from an Isuzu 1.7L diesel engine fuelled with ULSD. Whilst no explanation was provided for this observation, Chin et al. (2012) found the most abundant *n*-alkane shifted from *n*-nonane at idling conditions (800 rpm) with no load, to *n*-tridecane at 2500 rpm with maximum applied engine load (900 brake mean effective pressure, kPa).

The percentage contribution of the individual and grouped VOC-IVOCs to the ∑SpVOC emission rate in each experiment, is shown in Figure 4B. The percentage composition from a cold-start experiment (exp. 14) has also been included on the left of Figure 4B, to provide a comparison between cold idle engine conditions (which has a compositional profile most similar to unburnt fuel) and different engine loads. The percentage contribution of the individual and grouped VOC-IVOCs to the ∑SpVOC emissions changed considerably with different engine loads. All aromatics, except benzene, displayed a nonmonotonic behaviour with increasing engine load; their percentage contribution is high at cold idle and 40% load, with a smaller contribution at 30% and 53% load. This nonmonotonic behaviour has also been observed in Cross et. al. (2015). Cross et. al. (2015) investigated the load-dependant emissions from a 5.9L medium-duty diesel engine, fuelled with ULSD. It was found that the fractional contribution of oxidised species and aromatics (not explicitly mentioned but shown in the data) varied inconsistently with increasing engine load. The reason for this nonmonotonic behaviour is currently unclear. The percentage contribution of benzene generally decreased with increasing engine load. Interestingly, the percentage contribution of the *n*-alkanes continued to decrease from cold idle to 40% load, followed by a considerable increase at 53% load. At 53% load, the *n*-alkanes represented 55% of the ∑SpVOC emissions, 1.6 times greater than observed in the cold-start experiment.

Conversely, branched aliphatics displayed the opposite trend. The percentage contribution of the branched aliphatics continued to increase from cold idle to 40% load, followed by a considerable decrease at 53% load, to approximately the same percentage contribution observed in cold-start experiment.

This change in the percentage contribution of the *n*-alkanes and branched aliphatics at 53% engine load, can be explained by considering the DOC HC removal efficiency and the internal combustion temperature. The DOC HC removal efficiency is strongly dependant on working temperature. Below 200°C the DOC HC removal efficiency is close to zero, rising sharply to near 100% HC removal efficiency at ~ 430°C (Korin et al., 1999; Roberts et al., 2014; Majewski and Khair, 2006; Russell and Epling, 2011). From cold idle to 40% engine load, the engine temperature increased from < 100°C at cold idle, to 445°C at 40% load. The DOC HC removal efficiency is thus increasing from near zero at cold idle, to near maximum at 40% load. At 53% load, the steady-state engine temperature reached 700°C. The DOC HC removal efficiency was near maximum at 40% load and it is therefore unlikely that the DOC would account for such a considerable shift in the percentage contribution of the *n*-alkanes and branched aliphatics at 53% load. This shift in the composition is most likely the result of the considerably higher engine temperature, resulting in the fragmentation of higher molecular weight *n*-alkanes as a result of increased internal combustion efficiency. Straight-chain alkanes are more easily fragmented during combustion than branched aliphatics (Fox and Whitesell, 2004), resulting in a higher percentage contribution of smaller (*i.e.* C_7 to C_{12}) *n*-alkanes to the ∑SpVOC emissions at 53% load, in comparison to cold idle. The compositional profiles from 0 to 40% engine load, display the combined effect of increasing engine combustion efficiency and DOC HC removal efficiency, possibly explaining why a higher percentage contribution of C_7 to C_{12} *n*-alkanes is not observed with increasing engine load as a result of increasing engine combustion efficiency (*i.e.* DOC is likely masking the effect of increasing combustion efficiency on ∑SpVOC emissions).

3.3 DOC removal efficiency

The HC removal efficiency of the DOC was investigated by performing two repeat experiments (exp. 2 and 3, Table 1), with and without the DOC. The additional backpressure created due to the in-line DOC, appeared to have no effect on engine operation, allowing a direct comparison between experiments 2 and 3. The engine speed and load was set to 2500 rpm and 40% load, respectively. The steady-state engine temperature in both experiments was 450°C, the DOC was near maximum HC removal efficiency (Korin et al., 1999; Roberts et al., 2014; Majewski and Khair, 2006; Russell and Epling, 2011). The HC removal efficiency was calculated using the equation shown in Roberts et. al. (2013). The removal efficiency of the DOC for the speciated compounds is shown in Table 2. The DOC removed 46 ± 10 % of the ∑SpVOC emissions, with 83 ± 3 % for the single-ring aromatics and 39 ± 12 % for the aliphatics (branched and straight-chain). A typical DOC is expected to remove 50 to 70% of the total HC emissions (Johnson, 2001; Alam et al., 2016). For the investigated compounds, the total DOC removal efficiency is at the lower limit of this expectation. The DOC removal efficiency for styrene, m/p- and o-xylene, ethylbenzene (C_2 aromatic substitution grouping) and benzene, was greater than 90%. In addition, the trimethylbenzenes (TMB) were not observed with the use of the DOC (~ 100% removal efficiency). This high HC removal efficiency however, was not observed

for all the single-ring aromatics. Toluene had a relatively poor removal efficiency in comparison, at 59 ± 9 %. Furthermore, the removal efficiency of the unspeciated C_3 aromatic substitution grouping (*i.e.* less branched aromatic isomers of TMB) was determined to be 63 ± 22 %, suggesting the isomeric structure influences removal efficiency, possibly the result of reactivity and/or adsorption to the metal binding sites in the DOC (*c.f.* (Salge et al., 2005; Russell and Epling, 2011)).

Generally, the HC removal efficiency decreased with increasing carbon chain length. This was particularly evident with the branched aliphatics, with the removal efficiency decreasing from 72% to 14 % from C_7 to C_{12}, with a sharp decrease in the removal efficiency from C_{10} to C_{12}. Analogous to the branched aliphatics, the *n*-alkanes displayed the same rapid decrease in the HC removal efficiency between *n*-decane and *n*-dodecane, with the DOC observed to have no effect on the emission of *n*-dodecane. The removal of *n*-alkanes in the DOC have been found to decrease with increasing carbon chain length, a result of the greater number of adjacent sites in the DOC required to achieve absorption (Yao, 1980; Russell and Epling, 2011), supporting the results shown here. However, recently Alam et. al. (2016) investigated the HC removal efficiency of a similar specification DOC (*i.e.* mixed platinum and rhodium) for C_{12} to C_{33} *n*-alkanes, among other species. It was found that the DOC HC removal efficiency did not continue to decrease with increasing carbon chain length, rather decreasing from C_{12} to C_{16}, followed by an increase (C_{17} to C_{23}) and further decrease (C_{24} to C_{32}). Few studies have investigated the HC removal efficiency of individual species and grouped counterparts, expressing DOC HC removal efficiency as total HC, with no reference to possible compositional and structural effects, which based on the results shown in this study and Alam et. al. (2016), require further study.

3.4 Driving scenarios

The VOC-IVOC emission rates from several driving 'scenarios' were investigated. The driving scenarios included either; (i) a single applied engine load and speed, and injection before a steady-state engine temperature had been achieved (similar to transient conditions) or, (ii) a sequence of different engine loads and speeds, during which steady-state engine temperature was achieved. These experiments were performed to gain a greater insight into the factors controlling VOC-IVOC emission rates. Three experiments were performed, cold-start (exp. 6), cold loaded (exp. 8) and warm idle following load (WIFL, exp. 9). The sequence of engine conditions used in each of these experiments can be found in SI Figure S2. Cold loaded included a cold engine start followed by the immediate application of 1500 rpm and 20% load, with a one minute hold before injection. WIFL included a cold engine start, followed by the immediate application of 2000 rpm and 28-30% load with a 7-minute hold (during which a steady-state engine temperature was achieved), followed by one minute of idling speed (1150 rpm) and 0% load before injection. The ∑SpVOC emission rates in each experiment was 9268 ± 699, 2902 ± 199 and 1438 ± 96 mg kg^{-1} in the cold-start, cold loaded and WIFL, respectively. The application of 1500 rpm and 20% load for 1 minute (short-journey) resulted in a decrease in the ∑SpVOC emissions by a factor of ~ 3, in comparison to the cold-start engine conditions; highlighting the importance of engine combustion efficiency on VOC-IVOC emission rates. The VOC-IVOC emission rates and the exhaust composition in the investigated driving scenario experiments can be observed in Figure 5.

The engine temperature in the cold-start and cold loaded experiments was 85°C and 169°C, respectively. In the WIFL experiment, the engine temperature reached 290°C during steady-state, decreasing to 150°C upon injection. The ∑SpVOC emission rates were lower in the WIFL experiment than observed in the cold loaded experiment, where a higher engine temperature was measured upon injection. The HC removal efficiency of the DOC below 200°C is close to zero (Korin et al., 1999; Roberts et al., 2014; Majewski and Khair, 2006; Russell and Epling, 2011), suggesting the lower ∑SpVOC emissions observed in the WIFL experiment, is the result of increased combustion efficiency from the higher engine speed and load applied before idling conditions. Engine 'warm-up' increases the temperature of the lubricant, coolant and engine components, reducing friction and increasing combustion efficiency, thus resulting in less unburnt fuel emissions in the exhaust gas (*c.f.* (Roberts et al., 2014)). This increased combustion efficiency in the WIFL experiment is also supported by the exhaust gas composition (see Figure 5B). Considerably higher engine temperatures resulted in a greater proportion of higher molecular weight *n*-alkanes in the exhaust gas, an observation which could not be explained by the DOC and was attributed to combustion (see section 3.2). The engine temperatures in all three experiments were below 200°C and consequently, the DOC had a minimal effect on HC removal in these experiments. Therefore, the observed compositional changes in exhaust gas is the result of increasing combustion efficiency, which is supported by the sequential increase in the abundance of the *n*-alkanes as the internal combustion efficiency increases. The relationship between internal combustion efficiency and engine temperature is relatively linear (*e.g.*(Mikalsen and Roskilly, 2009)), with the exception of high engine loads and relatively low speeds (not performed here), where the engine combustion efficiency and temperature eventually plateau due to a too lean air/fuel ratio, resulting in incomplete combustion (see Haywood (1988) for further information). These experiments also provide additional information on the effect of the DOC on the exhaust gas emissions. In the engine load experiments (see section 3.2), the combined effect of increasing combustion efficiency and DOC HC removal efficiency on the exhaust gas emissions were observed from 0 to 40 % engine load, making it difficult to separate the effects of both factors on the exhaust gas composition. However, the observation of increasing *n*-alkane abundance with increasing engine combustion efficiency suggests that the increase in the abundance of the branched aliphatics at cold idle (exp. 14), 30% (exp. 12) and 40% load (exp. 13) (see section 3.2 and Figure 4B), respectively, is the result of the DOC fragmenting higher molecular weight branched aliphatics with increasing HC removal efficiency; indicating that the branched aliphatics are more easily fragmented in the DOC than *n*-alkanes, possibly the result of the fewer binding sites required in the DOC for adsorption.

The carbon number distribution of the branched aliphatics and *n*-alkanes in all three driving scenario experiments were comparable, dissimilar to the carbon number shift observed at high engine loads (*i.e.* 53% load). Furthermore, the nonmonatomic behaviour observed with the single-ring aromatics with increasing engine load was only observed with benzene. The percentage contribution of the C_3 aromatic substitution grouping to the ∑SpVOC emissions, displayed no obvious change with increasing combustion efficiency (within the calculated uncertainty). However, the abundance of the C_2 aromatic

substitution grouping and toluene generally decreased with increasing combustion efficiency, with the percentage contribution observed to plateau in the cold-start and cold loaded experiment, followed by a decrease in the WIFL experiment.

3.5 Atmospheric implications

The measured ∑SpVOC emission rates in each experiment (ordered from highest to lowest) are shown in Figure 6, along with the corresponding engine load, speed and temperature. The ∑SpVOC emission rates varied significantly with different engine conditions, ranging from 70 to 9268 mg kg^{-1}. The aliphatics represented 56 to 97% of the ∑SpVOC emission rates, with the single-ring aromatics accounting for the remainder. The highest ∑SpVOC emissions were observed in a cold-start experiment (exp. 6), with no applied load and idling speed (1150 rpm). Conversely, the lowest ∑SpVOC emissions were observed in the experiment with highest applied engine load and speed (exp. 11, 3000 rpm, 53% load). The ∑SpVOC emissions were observed to decrease with increasing engine load and temperature, and to a lesser degree, engine speed. This result is consistent with increased combustion efficiency and DOC HC removal efficiency with increasing temperature, similar to that observed in previous studies (*e.g.* (Cross et al., 2015; Chin et al., 2012)). The direct comparison of emission rates is difficult due to the vast number of differences between studies (*e.g.* types of speciated VOCs, vehicle types, emission control devices *etc.*). Furthermore, the majority of studies have investigated diesel exhaust emissions using chassis dynamometers, averaging emissions over entire driving cycles and often reporting emission rates as VOC mass per distance travelled; emissions and units which are not directly comparable with the emission rates shown here. The different types of instruments used to measure diesel exhaust emissions and the difficulties in the measurement of low volatility species, has in-part, resulted in considerable variation in the types of 'speciated' compounds between studies, making the direct comparison of emission rates extremely difficult. For example, Zhao et al. (2015) reported speciated and unspeciated IVOC emission rates from both medium-duty and heavy-duty diesel vehicles. In their study, speciated IVOCs included: straight and branched-chain alkanes, alkylcyclohexanes, unsubstituted and substituted polycyclic aromatic hydrocarbons and alkylbenzenes, with a volatility range of 10^2 to 10^6 µg m^{-3}. Similarly, Cross et al. (2015) measured IVOC emission rates from a medium-duty diesel engine. The emission rates reported in their study were based on compounds with a volatility range of ~ 10^3 to 10^7 µg m^{-3} and included cycloalkanes, bicycloalkanes, tricycloalkanes, straight and branched-chain aliphatics, and groupings of 'aromatics', 'oxidised' and 'remainder'. Moreover, Gordon et al. (2015) measured the emission rates of non-methane organic gases from medium-duty and heavy-duty diesel engines. In their study, speciated compounds included single-ring aromatics, straight and branched-chain aliphatics, cycloalkanes and non-aromatic carbonyls, with a volatility range of ~ 10^6 to 10^9µg m^{-3}. In this study, the emission rates from a light-duty diesel engine were reported, based on the emissions of straight and branched-chain aliphatics and single-ring aromatics, with a volatility range of ~ 10^5 to 10^8 µg m^{-3}. The investigated volatility range and chemical composition can have a considerable impact on the reported emission rates (*e.g.*(Zhao et al., 2015)). Whilst the above studies have comparable units to the emission rates shown in this work, emission rates have not been compared due to the differences in vehicular type (medium-duty and heavy-duty *vs.* light-duty) and the volatility and chemical composition of the speciated compounds. Further studies are required, providing emission rates of individually speciated compounds (where possible), to

facilitate direct comparison. Urban driving conditions are characterised by low engine speed, load and exhaust gas temperatures (*c.f.* (Franco et al., 2014; EEA, 2016)). Conversely, motorway or highway driving typically result in higher engine temperatures, due to increased engine speed and load. The results from this study show at low engine loads and speeds the emission rates of unregulated VOC-IVOCs per kilogram of fuel burnt, are considerably greater than emitted at higher engine speeds and loads. Furthermore, it was found that the exhaust gas composition varied depending primarily on combustion efficiency and DOC HC removal efficiency, both which are strongly dependent on working temperature (Korin et al., 1999; Roberts et al., 2014; Majewski and Khair, 2006; Russell and Epling, 2011). Diesel exhaust emissions contain thousands of compounds ranging from ~ C_5 to C_{22}, with contributions of up to C_{33} from lubricant oil (Alam et al., 2016; Gentner et al., 2017). Only a proportion of these emissions were speciated in this study. The measured compounds included aliphatics (branched and straight-chain) and single-ring aromatics with two and three carbon substituents, over a carbon range of C_6 to C_{13}. The narrow carbon range investigated is the result of instrument temperature constraints. The boiling points of compounds above ~ C_{15} are too high to be removed from the column at the maximum operating temperature of the modulator, resulting in these species not being detected. Of the measured compounds, branched aliphatics generally dominated the exhaust gas composition. However, at low engine temperatures (< 150°C), the proportion of *n*-alkanes in the exhaust gas were observed to increase with increasing combustion efficiency and could be important in urban environments; straight-chain alkanes are more efficient at producing SOA than their branched counterparts (Presto et al., 2010; Tkacik et al., 2012; Lim and Ziemann, 2009). Previous studies have suggested liquid fuel based emission factors are consistent with unburnt fuel in diesel exhaust emissions. For example, Gentner et al. (2013) showed the majority of VOC and IVOC diesel exhaust emissions were within 70% uncertainty of liquid fuel based emission factors. This work shows as combustion efficiency increases, the contribution of smaller, more volatile *n*-alkanes in the exhaust gas also increases, the result of increased fragmentation of higher molecular *n*-alkanes. This may suggest liquid diesel fuel based estimates of SOA yields may be inconsistent with diesel exhaust SOA yields, particularly at high engine temperatures (*i.e.* high engine loads and speeds). In recent years, emission regulations have focused on reducing NO_x emissions from diesel vehicles with the introduction of emission control technologies, such as exhaust gas recirculation (EGR), lean-burnt NO_x traps and selective catalytic reduction (Yang et al., 2015). To our knowledge, there are no further emission control technologies planned for the reduction of total hydrocarbon mass or unregulated VOCs. The emission rates from only one diesel engine was investigated in this study. However, several compositional changes in the exhaust gas were comparable with previous studies, suggesting compositional changes are relatively consistent between studies. The emission control devices used in this study were Euro 4 compliant. Euro 4 emission control regulations were first implemented for all new vehicles from approximately January 2006, with Euro 5 emission control regulations starting post January 2011. In the European Union (EU), ~ 27% of all on-road vehicles (both gasoline and petrol) were bought between 2006 to 2011 and thus conform to Euro 4 emission control regulations (ACEA, 2017). Of these vehicles, 75% are diesel (ACEA, 2017) and thus ~ 20% of the current EU diesel fleet are Euro 4 compliant. To our knowledge, this is the first study which has explicitly discussed the effect of the DOC HC removal efficiency and combustion efficiency on the exhaust gas composition. With further work, changes in exhaust gas composition as a function of engine temperature, could be

implemented into atmospheric models, improving model refinement and providing a better understanding of diesel exhaust emissions on local air quality.

Acknowledgments

The authors gratefully acknowledge the assistance of mechanical technicians Barry Gale and Lee Paul at the University of Manchester. This work was supported by NE/K012959/1 and NE/K014838/1.

4. References

Share of Diesel in New Passenger Cars: http://www.acea.be/statistics/tag/category/share-of-diesel-in-new-passenger-cars, access: 04/04/2017, 2016.

ACEA: ACEA Report: Vehicles in use Europe 2017, 2017.

Alam, M. S., Zeraati-Rezaei, S., Stark, C. P., Liang, Z., Xu, H., and Harrison, R. M.: The characterisation of diesel exhaust particles - composition, size distribution and partitioning, Faraday discussions, 189, 69-84, 10.1039/C5FD00185D, 2016.

Alkurdi, F., Karabet, F., and Dimashki, M.: Characterization, concentrations and emission rates of polycyclic aromatic hydrocarbons in the exhaust emissions from in-service vehicles in Damascus, Atmos Res, 120–121, 68-77, http://dx.doi.org/10.1016/j.atmosres.2012.08.003, 2013.

Alves, C. A., Lopes, D. J., Calvo, A. I., Evtyugina, M., Rocha, S., and Nunes, T.: Emissions from light-duty diesel and gasoline in-use vehicles measured on chassis dynamometer test cycles, Aerosol Air Qual Res, 15, 99-116, 2015.

Baldauf, R. W., Gabele, P., Crews, W., Snow, R., and Cook, J. R.: Criteria and Air-Toxic Emissions from In-Use Automobiles in the National Low-Emission Vehicle Program, Journal of the Air & Waste Management Association, 55, 1263-1268, 10.1080/10473289.2005.10464722, 2005.

Ballesteros, R., Guillén-Flores, J., and Martínez, J. D.: Carbonyl emission and toxicity profile of diesel blends with an animal-fat biodiesel and a tire pyrolysis liquid fuel, Chemosphere, 96, 155-166, https://doi.org/10.1016/j.chemosphere.2013.10.017, 2014.

Bohac, S. V., Han, M., Jacobs, T. J., López, A. J., Assanis, D. N., and Szymkowicz, P. G.: Speciated Hydrocarbon Emissions from an Automotive Diesel Engine and DOC Utilizing Conventional and PCI Combustion, 2006.

Caplain, I., Cazier, F., Nouali, H., Mercier, A., Déchaux, J.-C., Nollet, V., Joumard, R., André, J.-M., and Vidon, R.: Emissions of unregulated pollutants from European gasoline and diesel passenger cars, Atmospheric Environment, 40, 5954-5966, http://dx.doi.org/10.1016/j.atmosenv.2005.12.049, 2006.

Chin, J.-Y., Batterman, S. A., Northrop, W. F., Bohac, S. V., and Assanis, D. N.: Gaseous and Particulate Emissions from Diesel Engines at Idle and under Load: Comparison of Biodiesel Blend and Ultralow Sulfur Diesel Fuels, Energy & Fuels, 26, 6737-6748, 10.1021/ef300421h, 2012.

Chirico, R., Clairotte, M., Adam, T. W., Giechaskiel, B., Heringa, M. F., Elsasser, M., Martini, G., Manfredi, U., Streibel, T., Sklorz, M., Zimmermann, R., DeCarlo, P. F., Astorga, C., Baltensperger, U., and Prevot, A. S. H.: Emissions of organic aerosol mass, black carbon, particle number, and regulated and unregulated gases from scooters and light and heavy duty vehicles with different fuels, Atmos. Chem. Phys. Discuss., 2014, 16591-16639, 10.5194/acpd-14-16591-2014, 2014.

Cohen, A. J., Ross Anderson, H., Ostro, B., Pandey, K. D., Krzyzanowski, M., Künzli, N., Gutschmidt, K., Pope, A., Romieu, I., Samet, J. M., and Smith, K.: The Global Burden of Disease Due to Outdoor Air Pollution, Journal of Toxicology and Environmental Health, Part A, 68, 1301-1307, 10.1080/15287390590936166, 2005.

Colvile, R., Hutchinson, E., Mindell, J., and Warren, R.: The transport sector as a source of air pollution, Atmospheric environment, 35, 1537-1565, 2001.

Cross, E. S., Sappok, A. G., Wong, V. W., and Kroll, J. H.: Load-Dependent Emission Factors and Chemical Characteristics of IVOCs from a Medium-Duty Diesel Engine, Environmental science & technology, 49, 13483-13491, 10.1021/acs.est.5b03954, 2015.

de Gouw, J. A., Middlebrook, A. M., Warneke, C., Goldan, P. D., Kuster, W. C., Roberts, J. M., Fehsenfeld, F. C., Worsnop, D. R., Canagaratna, M. R., Pszenny, A. A. P., Keene, W. C., Marchewka, M., Bertman, S. B., and Bates, T. S.: Budget of organic carbon in a polluted atmosphere: Results from the New England Air Quality Study in 2002, Journal of Geophysical Research: Atmospheres, 110, n/a-n/a, 10.1029/2004JD005623, 2005.

DEFA: Diesel Vehicle Emissions and Urban Air Quality - Second QUARG report, 1993.

Donahue, N., Robinson, A., Stanier, C., and Pandis, S.: Coupled partitioning, dilution, and chemical aging of semivolatile organics, Environmental science & technology, 40, 2635-2643, 2006.

Dunmore, R. E., Hopkins, J. R., Lidster, R. T., Lee, J. D., Evans, M. J., Rickard, A. R., Lewis, A. C., and Hamilton, J. F.: Diesel-related hydrocarbons can dominate gas phase reactive carbon in megacities, Atmos. Chem. Phys., 15, 9983-9996, 10.5194/acp-15-9983-2015, 2015.

EEA: Explaining road transport emissions, 22, 2016.

EU: Offical Journal of the European Union: Directive 2009/30/EC, L 140/88, 2009.

Fox, M., and Whitesell, J.: Organic Chemistry, Third ed., Jones and Bartlett, London, 1140 pp., 2004.

Franco, V., Sánchez, F. P., German, J., and Mock, P.: Real-world exhaust emissions from modern diesel cars, 8, 2014.

Fraser, M. P., Cass, G. R., and Simoneit, B. R. T.: Gas-Phase and Particle-Phase Organic Compounds Emitted from Motor Vehicle Traffic in a Los Angeles Roadway Tunnel, Environmental science & technology, 32, 2051-2060, 10.1021/es970916e, 1998.

Gentner, D. R., Worton, D. R., Isaacman, G., Davis, L. C., Dallmann, T. R., Wood, E. C., Herndon, S. C., Goldstein, A. H., and Harley, R. A.: Chemical Composition of Gas-Phase Organic Carbon Emissions from Motor Vehicles and Implications for Ozone Production, Environmental science & technology, 47, 11837-11848, 10.1021/es401470e, 2013.

Gentner, D. R., Jathar, S. H., Gordon, T. D., Bahreini, R., Day, D. A., El Haddad, I., Hayes, P. L., Pieber, S. M., Platt, S. M., de Gouw, J., Goldstein, A. H., Harley, R. A., Jimenez, J. L., Prévôt, A. S. H., and Robinson, A. L.: Review of Urban Secondary

Organic Aerosol Formation from Gasoline and Diesel Motor Vehicle Emissions, Environmental science & technology, 51, 1074-1093, 10.1021/acs.est.6b04509, 2017.

Gordon, T. D., Presto, A. A., Nguyen, N. T., Robertson, W. H., Na, K., Sahay, K. N., Zhang, M., Maddox, C., Rieger, P., Chattopadhyay, S., Maldonado, H., Maricq, M. M., and Robinson, A. L.: Secondary organic aerosol production from diesel vehicle exhaust: impact of aftertreatment, fuel chemistry and driving cycle, Atmos. Chem. Phys., 14, 4643-4659, 10.5194/acp-14-4643-2014, 2014.

Hallquist, M., Wenger, J. C., Baltensperger, U., Rudich, Y., Simpson, D., Claeys, M., Dommen, J., Donahue, N. M., George, C., Goldstein, A. H., Hamilton, J. F., Herrmann, H., Hoffmann, T., Iinuma, Y., Jang, M., Jenkin, M. E., Jimenez, J. L., Kiendler-Scharr, A., Maenhaut, W., McFiggans, G., Mentel, T. F., Monod, A., Prévôt, A. S. H., Seinfeld, J. H., Surratt, J. D., Szmigielski, R., and J., W.: The formation, properties and impact of secondary organic aerosol: current and emerging issues, Atmos Chem Phys, 9, 5155-5236, 2009.

Han, X., and Naeher, L. P.: A review of traffic-related air pollution exposure assessment studies in the developing world, Environment International, 32, 106-120, http://dx.doi.org/10.1016/j.envint.2005.05.020, 2006.

HEI: Traffic-Related Air Pollution: A Critical Review of the Literature on Emissions, Exposure, and Health Effects, 2010.

Heywood, J. B.: Internal combustion engine fundamentals, Mcgraw-hill New York, 1988.

Ježek, I., Katrašnik, T., Westerdahl, D., and Močnik, G.: Black carbon, particle number concentration and nitrogen oxide emission factors of random in-use vehicles measured with the on-road chasing method, Atmos. Chem. Phys., 15, 11011-11026, 10.5194/acp-15-11011-2015, 2015.

Jiang, M., Marr, L. C., Dunlea, E. J., Herndon, S. C., Jayne, J. T., Kolb, C. E., Knighton, W. B., Rogers, T. M., Zavala, M., Molina, L. T., and Molina, M. J.: Vehicle fleet emissions of black carbon, polycyclic aromatic hydrocarbons, and other pollutants measured by a mobile laboratory in Mexico City, Atmos. Chem. Phys., 5, 3377-3387, 10.5194/acp-5-3377-2005, 2005.

Johnson, T. V.: Diesel Emission Control in Review, 2001.

Kondo, Y., Miyazaki, Y., Takegawa, N., Miyakawa, T., Weber, R. J., Jimenez, J. L., Zhang, Q., and Worsnop, D. R.: Oxygenated and water-soluble organic aerosols in Tokyo, Journal of Geophysical Research: Atmospheres, 112, n/a-n/a, 10.1029/2006JD007056, 2007.

Korin, E., Reshef, R., Tshernichovesky, D., and Sher, E.: Reducing cold-start emission from internal combustion engines by means of a catalytic converter embedded in a phase-change material, Proceedings of the Institution of Mechanical Engineers, Part D: Journal of Automobile Engineering, 213, 575-583, doi:10.1243/0954407991527116, 1999.

Kristensson, A., Johansson, C., Westerholm, R., Swietlicki, E., Gidhagen, L., Wideqvist, U., and Vesely, V.: Real-world traffic emission factors of gases and particles measured in a road tunnel in Stockholm, Sweden, Atmospheric Environment, 38, 657-673, http://dx.doi.org/10.1016/j.atmosenv.2003.10.030, 2004.

Krzyzanowski, M., and Cohen, A.: Update of WHO air quality guidelines, Air Quality, Atmosphere & Health, 1, 7-13, 10.1007/s11869-008-0008-9, 2008.

Lidster, R. T.: Development of comprehensive two-dimensional gas chromatography for the analysis of volatile organic compounds in the atmosphere, University of York, 2012.

Lim, Y. B., and Ziemann, P. J.: Effects of Molecular Structure on Aerosol Yields from OH Radical-Initiated Reactions of Linear, Branched, and Cyclic Alkanes in the Presence of NOx, Environmental science & technology, 43, 2328-2334, 10.1021/es803389s, 2009.

Liu, Y., Gao, Y., Yu, N., Zhang, C., Wang, S., Ma, L., Zhao, J., and Lohmann, R.: Particulate matter, gaseous and particulate polycyclic aromatic hydrocarbons (PAHs) in an urban traffic tunnel of China: Emission from on-road vehicles and gas-particle partitioning, Chemosphere, 134, 52-59, http://dx.doi.org/10.1016/j.chemosphere.2015.03.065, 2015.

Louis, C., Liu, Y., Tassel, P., Perret, P., Chaumond, A., and André, M.: PAH, BTEX, carbonyl compound, black-carbon, NO2 and ultrafine particle dynamometer bench emissions for Euro 4 and Euro 5 diesel and gasoline passenger cars, Atmospheric Environment, 141, 80-95, http://dx.doi.org/10.1016/j.atmosenv.2016.06.055, 2016.

Machado Corrêa, S., and Arbilla, G.: Carbonyl emissions in diesel and biodiesel exhaust, Atmospheric Environment, 42, 769-775, https://doi.org/10.1016/j.atmosenv.2007.09.073, 2008.

Majewski, W. A., and Khair, M. K.: Diesel emissions and their control, SAE Technical Paper, 2006.

Matsui, H., Koike, M., Takegawa, N., Kondo, Y., Griffin, R. J., Miyazaki, Y., Yokouchi, Y., and Ohara, T.: Secondary organic aerosol formation in urban air: Temporal variations and possible contributions from unidentified hydrocarbons, Journal of Geophysical Research: Atmospheres, 114, n/a-n/a, 10.1029/2008JD010164, 2009.

Miguel, A. H., Kirchstetter, T. W., Harley, R. A., and Hering, S. V.: On-Road Emissions of Particulate Polycyclic Aromatic Hydrocarbons and Black Carbon from Gasoline and Diesel Vehicles, Environmental science & technology, 32, 450-455, 10.1021/es970566w, 1998.

Nelson, P. F., Tibbett, A. R., and Day, S. J.: Effects of vehicle type and fuel quality on real world toxic emissions from diesel vehicles, Atmospheric Environment, 42, 5291-5303, https://doi.org/10.1016/j.atmosenv.2008.02.049, 2008.

Pang, Y., Fuentes, M., and Rieger, P.: Trends in the emissions of Volatile Organic Compounds (VOCs) from light-duty gasoline vehicles tested on chassis dynamometers in Southern California, Atmospheric Environment, 83, 127-135, http://dx.doi.org/10.1016/j.atmosenv.2013.11.002, 2014.

Presto, A. A., Miracolo, M. A., Donahue, N. M., and Robinson, A. L.: Secondary Organic Aerosol Formation from High-NOx Photo-Oxidation of Low Volatility Precursors: n-Alkanes, Environmental science & technology, 44, 2029-2034, 10.1021/es903712r, 2010.

Prüss-Üstün, A., and Corvalán, C.: Preventing disease through healthy environments, Geneva: World Health Organization, 2006.

Rashid, G., Hekmat, R., Nejat, L. A., Payam, J., and Farzad, J.: Comparative analysis of exhaust gases from MF285 and U650 tractors under field conditions, Agricultural Engineering International: CIGR Journal, 15, 101-107, 2013.

Roberts, A., Brooks, R., and Shipway, P.: Internal combustion engine cold-start efficiency: A review of the problem, causes and potential solutions, Energy Conversion and Management, 82, 327-350, http://dx.doi.org/10.1016/j.enconman.2014.03.002, 2014.

Russell, A., and Epling, W. S.: Diesel Oxidation Catalysts, Catalysis Reviews, 53, 337-423, 10.1080/01614940.2011.596429, 2011.

Salge, J., Deluga, G., and Schmidt, L.: Catalytic partial oxidation of ethanol over noble metal catalysts, Journal of Catalysis, 235, 69-78, 2005.

Schauer, J. J., Kleeman, M. J., Cass, G. R., and Simoneit, B. R. T.: Measurement of Emissions from Air Pollution Sources. 2. C1 through C30 Organic Compounds from Medium Duty Diesel Trucks, Environmental science & technology, 33, 1578-1587, 10.1021/es980081n, 1999.

Schmitz, T., Hassel, D., and Weber, F.-J.: Determination of VOC-components in the exhaust of gasoline and diesel passenger cars, Atmospheric Environment, 34, 4639-4647, http://dx.doi.org/10.1016/S1352-2310(00)00303-4, 2000.

Schulz, H., Bandeira De Melo, G., and Ousmanov, F.: Volatile organic compounds and particulates as components of diesel engine exhaust gas, Combustion and Flame, 118, 179-190, https://doi.org/10.1016/S0010-2180(98)00146-1, 1999.

Shirneshan, A.: HC, CO, CO2 and NOx Emission Evaluation of a Diesel Engine Fueled with Waste Frying Oil Methyl Ester, Procedia - Social and Behavioral Sciences, 75, 292-297, http://dx.doi.org/10.1016/j.sbspro.2013.04.033, 2013.

Siegl, W. O., Hammerle, R. H., Herrmann, H. M., Wenclawiak, B. W., and Luers-Jongen, B.: Organic emissions profile for a light-duty diesel vehicle, Atmospheric Environment, 33, 797-805, https://doi.org/10.1016/S1352-2310(98)00209-X, 1999.

Staehelin, J., Keller, C., Stahel, W., Schläpfer, K., and Wunderli, S.: Emission factors from road traffic from a tunnel study (Gubrist tunnel, Switzerland). Part III: Results of organic compounds, SO2 and speciation of organic exhaust emission, Atmospheric Environment, 32, 999-1009, https://doi.org/10.1016/S1352-2310(97)00339-7, 1998.

Tadano, Y. S., Borillo, G. C., Godoi, A. F. L., Cichon, A., Silva, T. O. B., Valebona, F. B., Errera, M. R., Penteado Neto, R. A., Rempel, D., Martin, L., Yamamoto, C. I., and Godoi, R. H. M.: Gaseous emissions from a heavy-duty engine equipped with SCR aftertreatment system and fuelled with diesel and biodiesel: Assessment of pollutant dispersion and health risk, Science of The Total Environment, 500–501, 64-71, http://dx.doi.org/10.1016/j.scitotenv.2014.08.100, 2014.

Takegawa, N., Miyakawa, T., Kondo, Y., Blake, D. R., Kanaya, Y., Koike, M., Fukuda, M., Komazaki, Y., Miyazaki, Y., Shimono, A., and Takeuchi, T.: Evolution of submicron organic aerosol in polluted air exported from Tokyo, Geophysical Research Letters, 33, n/a-n/a, 10.1029/2006GL025815, 2006.

Tkacik, D. S., Presto, A. A., Donahue, N. M., and Robinson, A. L.: Secondary Organic Aerosol Formation from Intermediate-Volatility Organic Compounds: Cyclic, Linear, and Branched Alkanes, Environmental science & technology, 46, 8773-8781, 10.1021/es301112c, 2012.

UnitedNations: World Urbanization Prospects: The 2014 Revision, Highlights. Department of Economic and Social Affairs, Population Division, United Nations, 2014.

Volkamer, R., Jimenez, J. L., San Martini, F., Dzepina, K., Zhang, Q., Salcedo, D., Molina, L. T., Worsnop, D. R., and Molina, M. J.: Secondary organic aerosol formation from anthropogenic air pollution: Rapid and higher than expected, Geophysical Research Letters, 33, n/a-n/a, 10.1029/2006GL026899, 2006.

Westerholm, R. N., Almen, J., Li, H., Rannug, J. U., Egebaeck, K. E., and Graegg, K.: Chemical and biological characterization of particulate-, semivolatile-, and gas-phase-associated compounds in diluted heavy-duty diesel exhausts: a comparison of three different semivolatile-phase samplers, Environmental science & technology, 25, 332-338, 10.1021/es00014a018, 1991.

WHO: World Health Organization Air quality guidelines for particulate matter, ozone, nitrogen dioxide and sulfur dioxide: global update 2005: summary of risk assessment, 2006.

Williams, P. I., McFiggans, G., and Gallagher, M. W.: Latitudinal aerosol size distribution variation in the Eastern Atlantic Ocean measured aboard the FS-Polarstern, Atmos. Chem. Phys., 7, 2563-2573, 10.5194/acp-7-2563-2007, 2007.

Winklmayr, W., Reischl, G. P., Lindner, A. O., and Berner, A.: A new electromobility spectrometer for the measurement of aerosol size distributions in the size range from 1 to 1000 nm, Journal of Aerosol Science, 22, 289-296, http://dx.doi.org/10.1016/S0021-8502(05)80007-2, 1991.

Yamada, H., Misawa, K., Suzuki, D., Tanaka, K., Matsumoto, J., Fujii, M., and Tanaka, K.: Detailed analysis of diesel vehicle exhaust emissions: Nitrogen oxides, hydrocarbons and particulate size distributions, Proceedings of the Combustion Institute, 33, 2895-2902, http://dx.doi.org/10.1016/j.proci.2010.07.001, 2011.

Yang, L., Franco, V., Mock, P., Kolke, R., Zhang, S., Wu, Y., and German, J.: Experimental Assessment of NOx Emissions from 73 Euro 6 Diesel Passenger Cars, Environmental science & technology, 49, 14409-14415, 10.1021/acs.est.5b04242, 2015.

Yao, Y.-F. Y.: Oxidation of Alkanes over Noble Metal Catalysts, Industrial & Engineering Chemistry Product Research and Development, 19, 293-298, 10.1021/i360075a003, 1980.

Zavala, M., Herndon, S. C., Slott, R. S., Dunlea, E. J., Marr, L. C., Shorter, J. H., Zahniser, M., Knighton, W. B., Rogers, T. M., Kolb, C. E., Molina, L. T., and Molina, M. J.: Characterization of on-road vehicle emissions in the Mexico City Metropolitan Area using a mobile laboratory in chase and fleet average measurement modes during the MCMA-2003 field campaign, Atmos. Chem. Phys., 6, 5129-5142, 10.5194/acp-6-5129-2006, 2006.

Zhao, Y., Nguyen, N. T., Presto, A. A., Hennigan, C. J., May, A. A., and Robinson, A. L.: Intermediate Volatility Organic Compound Emissions from On-Road Diesel Vehicles: Chemical Composition, Emission Factors, and Estimated Secondary Organic Aerosol Production, Environmental science & technology, 49, 11516-11526, 10.1021/acs.est.5b02841, 2015.

Zhu, L., Cheung, C. S., Zhang, W. G., Fang, J. H., and Huang, Z.: Effects of ethanol–biodiesel blends and diesel oxidation catalyst (DOC) on particulate and unregulated emissions, Fuel, 113, 690-696, https://doi.org/10.1016/j.fuel.2013.06.028, 2013.

Table 1 – Experimental dates, descriptions and engine operating parameters.

Experiment	Experiment Date	Experiment Description	Engine Conditions							Exhaust dilution ratio	Exhaust emission†		
			RPM	Throttle (%)	Load (%)	Torque (Nm)	DOC	Engine Temp (°C)	Fuel Burnt (g)		NO ($g\ kg^{-1}$)	NO_2 ($g\ kg^{-1}$)	Particle mass ($mg\ kg^{-1}$)⁜
1	30.07.14	Warm high load[a]	2500	57	40	75	Yes	460	6.13	166	27.6	3.2	302
2	31.07.14	Warm high load[a]	2500	57	40	75	Yes	450	2.45	313	23.4	1.9	235
3	01.08.14	Warm high load	2500	57	40	75	No	450	2.45	325	21.7	2.5	198
4	05.08.14	Warm with load[b]	2000	40	30	50	Yes	**	0.41	1158	26.1	0.5	220
5	08.08.14	Warm with load[b]	2000	40	30	50	Yes	300	8.27	60	20.7	3.1	268
6	06.08.14	Cold Start[c]	1150	0	0	1.5	Yes	85	0.59	389	7.2	15.0	1159
7	07.08.14	Cold Start[c]	1150	0	0	2	Yes	83	0.59	564***	7.9	14.6	915
8	06.08.14 (2)	Cold loaded*	1500	30	20	32	Yes	169	1.19	312	17.3	9.8	121
9	06.08.14 (3)	Warm idle following load*	1180	0	0	0.3	Yes	150	1.18	775	13.1	0.9	168
10	13.11.14 (1)	Warm with load[b]	2000	40	30	50	Yes	300	0.41	840	31.5	2.0	351
11	13.11.14 (2)	High RPM, 53% load	3000	75	53	112	Yes	700	3.28	353	21.7	1.9	2146
12	14.11.14 (1)	High RPM, 30% load	3000	48	30	50	Yes	345	1.74	198	39.2	5.3	600
13	14.11.14 (2)	High RPM, 40% load	3000	57	40	70	Yes	445	2.39	191	44.6	8.6	655
14	25.11.14	Cold Start[c]	1150	0	0	2	Yes	**	0.59	564***	6.3	10.6	1159
15	01.10.15	Warm with load[b]	2000	40	28	50	Yes	292	1.57	331	12.8	0.5	298
16	29.09.15	Warm with load[b]	2000	40	28	50	Yes	293	1.57	337	12.2	0.5	241

Superscript letters a, b and c highlight replicate experiments using the same engine conditions. Fuel batch A used in experiments 1 to 9 and fuel batch B, used in experiments 10 to 16, see section 2.2 and 3.1.1 for further information. *= Sequence of engine conditions performed, see section 2.3 and SI Figure S2. **No engine temperature measurement (engine thermocouple non-responsive). ***Estimated exhaust dilution ratio based on pneumatic valve introduction time. †Expressed as emission factors (*i.e.* mass of emission per kg of fuel burnt). ⁜Wall loss corrected.

Table 2 – Calculated diesel oxidative catalyst hydrocarbon removal efficiency for the speciated VOCs. Determined from measured emissions rates of the speciated VOCs in two replicate experiments with (exp. 2) and without (exp. 3) a diesel oxidative catalyst.

	Emission without catalytic converter (mg kg^{-1})	Emission with catalytic converter (mg kg^{-1})	Removal efficiency (%)
Individual Compounds			
Benzene	19.50±1.75	1.88±0.17	90.4±9.0
Toluene	3.89±0.37	1.58±0.15	59.3±9.4
Ethyl benzene	1.56±0.36	0.05±0.01	97.1±22.8
m/p-xylene	2.98±0.62	0.13±0.03	95.7±20.9
o-xylene	2.17±0.55	0.22±0.06	89.7±25.3
Styrene	2.74±0.69	0.01±0.004	99.5±25.3
1,3,5-TMB	2.26±0.36	0	100*
1,2,4-TMB	2.45±0.21	0	100*
1,2,3-TMB	1.92±0.20	0	100*
Heptane	2.37±0.14	0.53±0.03	77.4±5.7
Octane	4.96±0.57	0	100*
Nonane	11.72±1.08	2.44±0.22	79.2±9.2
Decane	33.83±3.11	7.30±0.67	78.4±9.2
Undecane	49.76±4.57	32.34±2.97	35.0±9.2
Dodecane	137.65±12.64	156.60±14.38	0**
Groupings			
Branched aliphatics			
C_7	4.41±1.00	1.25±0.28	71.6±22.6
C_8	18.77±4.76	3.68±0.93	80.4±25.4
C_9	46.78±10.70	6.65±1.52	85.8±22.9
C_{10}	76.81±18.78	17.33±4.24	77.4±24.4
C_{11}	71.95±16.43	31.97±7.30	55.6±22.8
C_{12}	86.36±20.80	74.41±17.92	13.8±24.1
Aromatic substitutions			
C_3	14.18±3.13	5.20±1.15	63.3±22.1
Total groupings			
Aliphatics	545.37±37.22	334.50±24.74	38.66±11.7
Aromatics	53.65±3.81	9.07±1.17	83.09±2.6
Total speciated	599.02±37.41	343.58±24.77	45.64±9.7

* Compound not observed (< instrument LOD). **No observed decrease in concentration. TMB = trimethyl benzene.

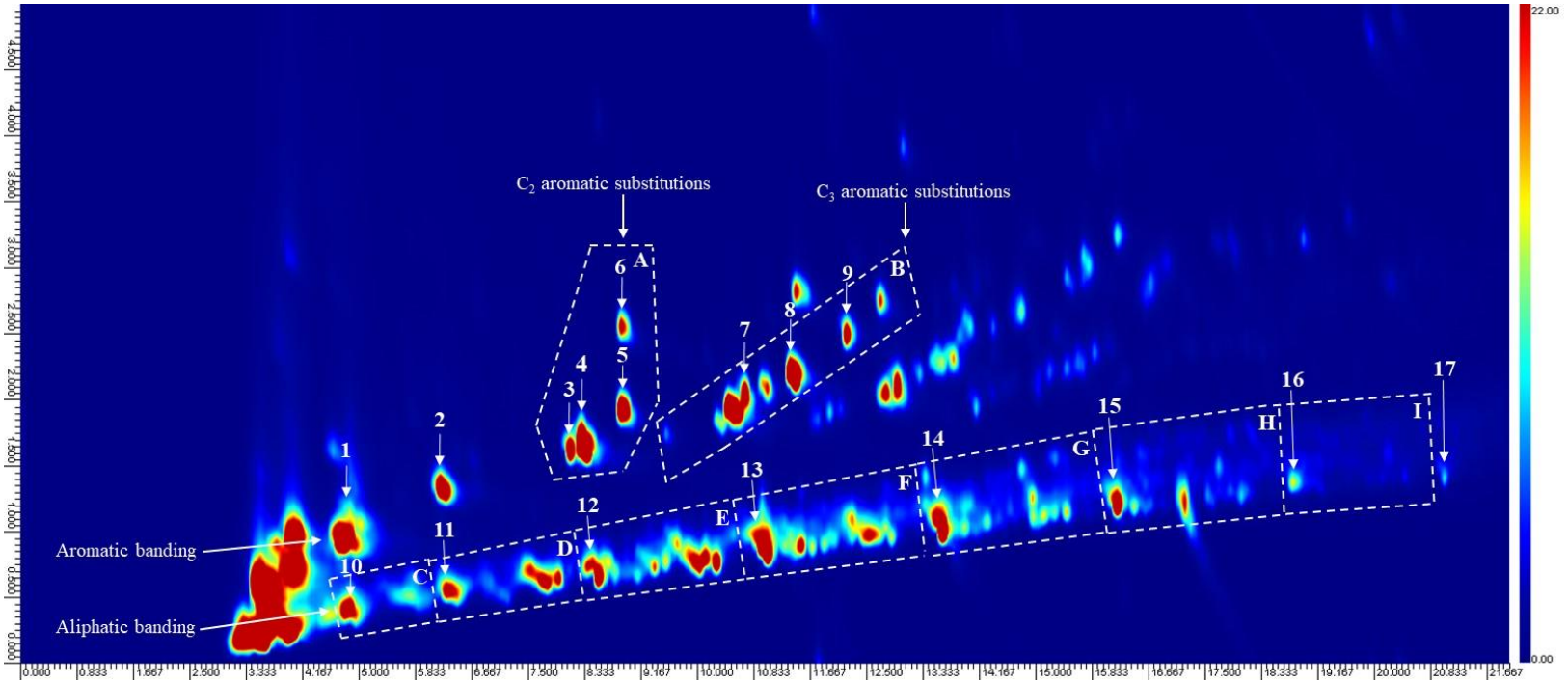

Figure 1 – An annotated chromatogram displaying the speciated VOC-IVOCs. Chromatogram axis, x = first dimension separation (boiling point, increasing from left-to-right), y = second dimension separation (polarity, increasing from bottom-to-top). Colour scale represents peak intensity, increasing from blue to red. Letters refer to compound groupings; A = single-ring aromatics with two carbon substitutions, B = single-ring aromatics with three carbon substitutions, C to I = C_7 to C_{13} aliphatics grouped by carbon number (*i.e.* C = C_7 aliphatics, D = C_8 aliphatics *etc.*). Numbers refer to individual compounds; 1 = benzene, 2 = toluene, 3 = ethyl benzene, 4 = meta/para-xylene (co-elution), 5 = ortho-xylene, 6 = styrene, 7 = 1,3,5-trimethyl benzene, 8 = 1,2,4-trimethyl benzene, 9 = 1,2,3-trimethyl benzene, 10 = heptane, 11= octane, 12 = nonane, 13 = decane, 14 = undecane, 15 = dodecane, 16 = tridecane, 17 = tetradecane (not quantified). Aromatic and aliphatic bandings often observed with this technique are shown (*c.f.* Hamilton and Lewis (2003) and Dunmore et al. (2015)). The start and end of each aliphatic grouping is marked by the lower and higher carbon number *n*-alkane (*i.e.* nonane marks the start of the C_9 aliphatic grouping, decane marks the end of this group).

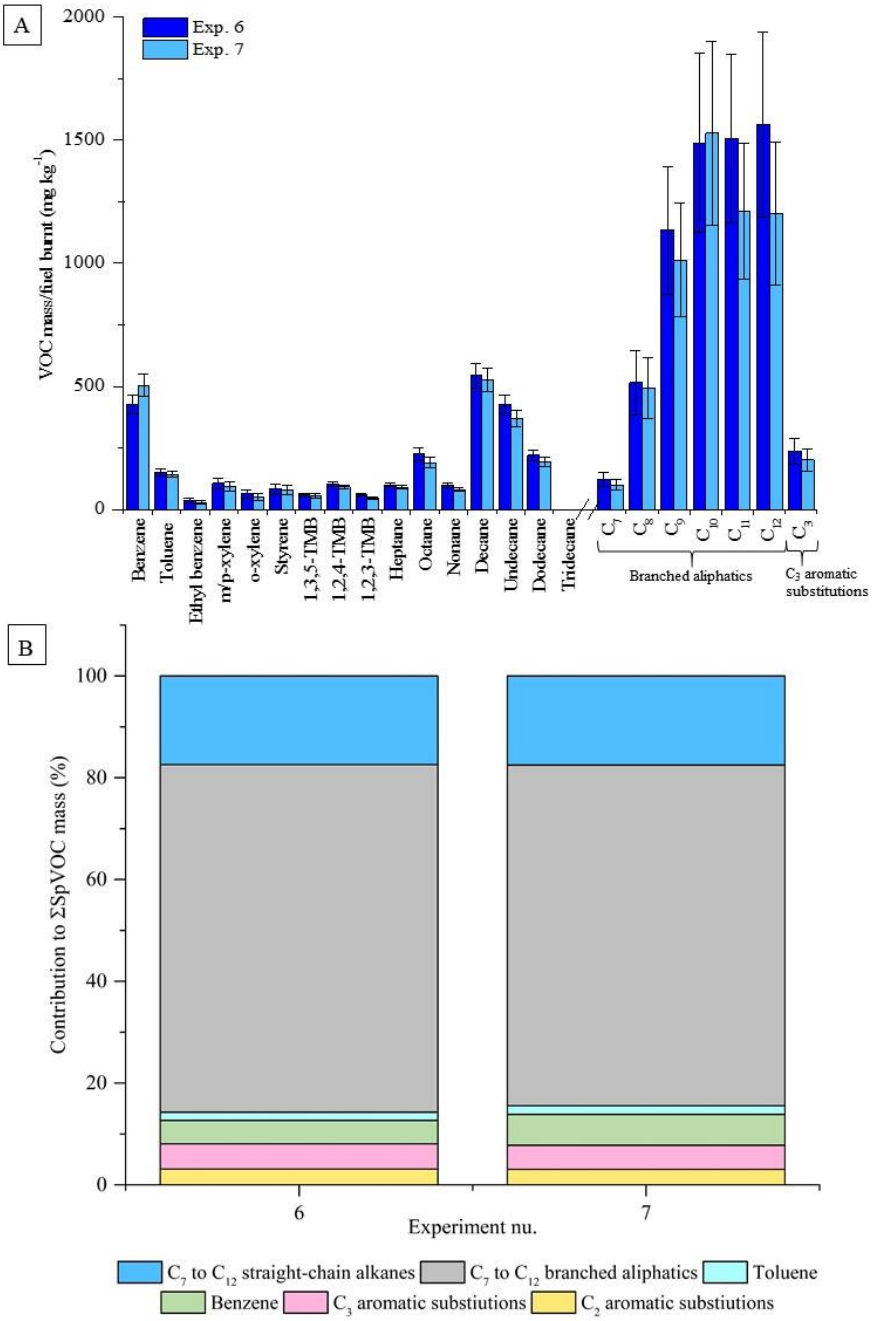

Figure 2 – Comparison of measured VOC-IVOC emission rates in replicate cold-start experiments (exp. 6 and 7) (A). Comparison of the percentage contribution of the individual and grouped compounds to the ∑SpVOC emission rates in exp. 6 and 7 (B). The emission rates of tridecane and the C_{13} branched aliphatic grouping has not been included in (B) to allow direct comparison between other experiments where these species were not measured. Error bars represent the calculated uncertainty in the measured emission rates, see the SI section 1.1 for further information.

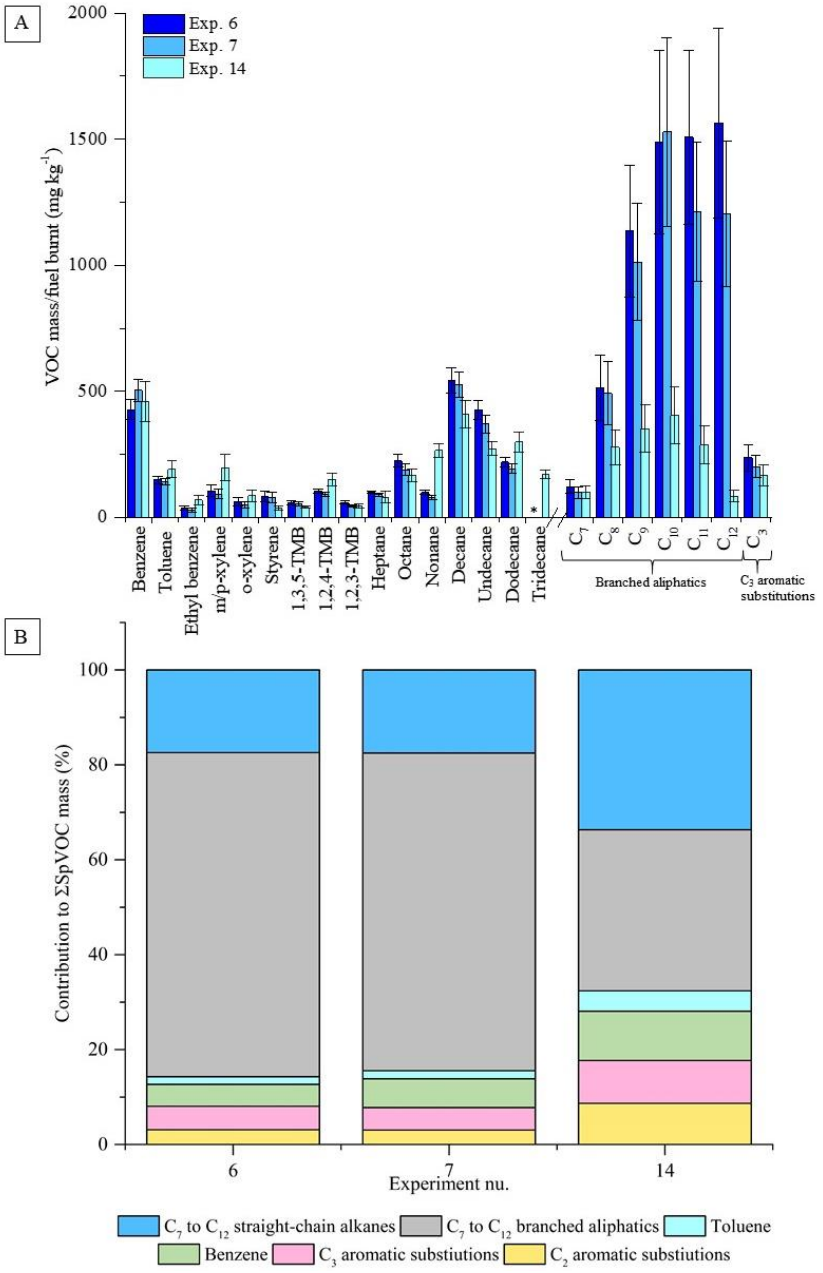

Figure 3 – Comparison of measured VOC-IVOC emissions rates in replicate cold-start experiments 6 and 7 (fuel batch A) with cold-start experiment 14 (fuel batch B) (A). Comparison of the percentage contribution of the individual and grouped compounds to the ∑SpVOC emission rates in experiments 6, 7, 14 (B). The emission rates of tridecane and the C_{13} branched aliphatic grouping has not been included in (B) to allow direct comparison between other experiments where these species were not measured. Error bars represent the calculated uncertainty in the measured emission rates, see the SI section 1.1 for further information.

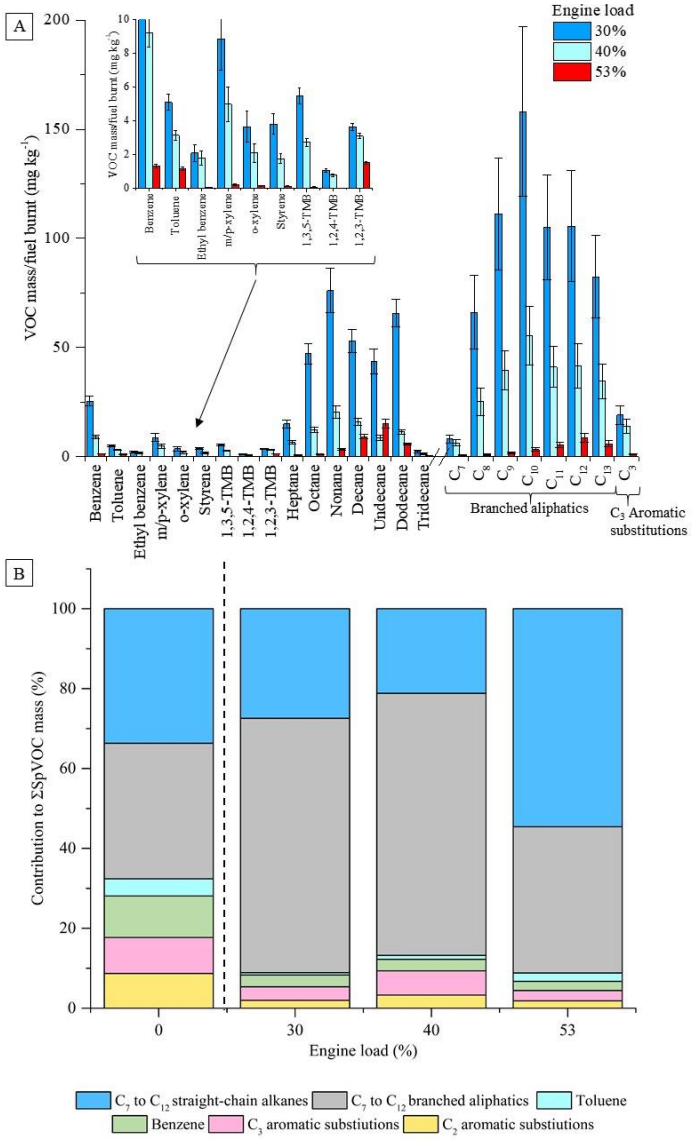

Figure 4 – Effect of different engine loads on measured VOC-IVOC emission rates (A) and the percentage contribution of the individual and grouped compounds to the ∑SpVOC emission rate at 0 (exp. 14), 30 (exp. 12), 40 (exp. 13) and 53% (exp. 11) engine load (B). The emission rates of tridecane and the C_{13} branched aliphatic grouping have not been included in (B) to allow direct comparison between other experiments where these species were not measured. For comparison, the percentage contribution of the individual and grouped compounds to the ∑SpVOC emission rate in a cold idle experiment (exp. 14) has been included on the left of (B), see text for further details. Error bars represent the calculated uncertainty in the measured emission rates, see the SI section 1.1 for further information.

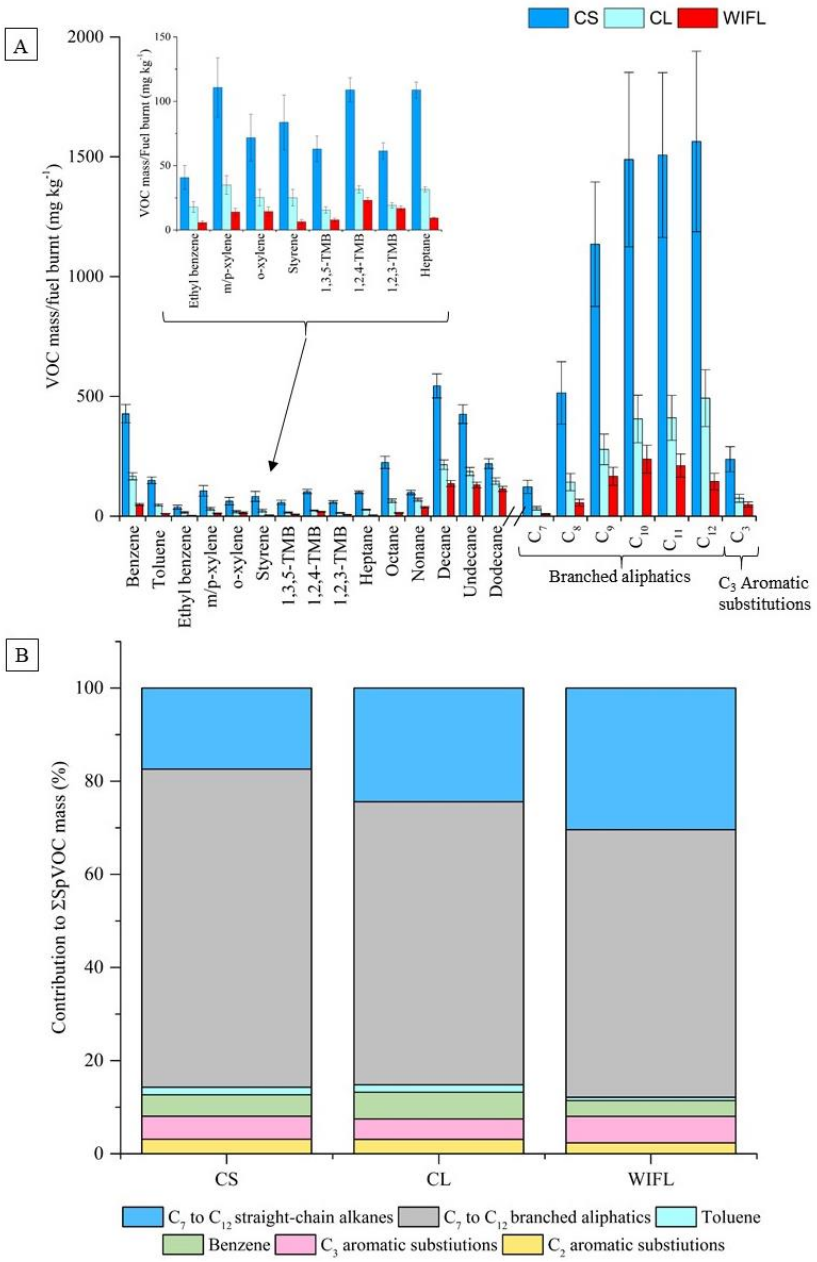

Figure 5 – Effect of different driving scenarios on measured VOC-IVOC emission rates (A) and the contribution of the individual and grouped compounds to the ∑SpVOC emission rate (B). CS = cold-start (exp. 6). SJ = cold loaded (exp. 8), WIFL = warm idle following load (exp. 9, see text for further information). The emission rates of tridecane and the C_{13} branched aliphatic grouping have not been included in (B) to allow direct comparison between other experiments where these species were not measured. Error bars represent the calculated uncertainty in the measured emission rates, see the SI section 1.1 for further information.

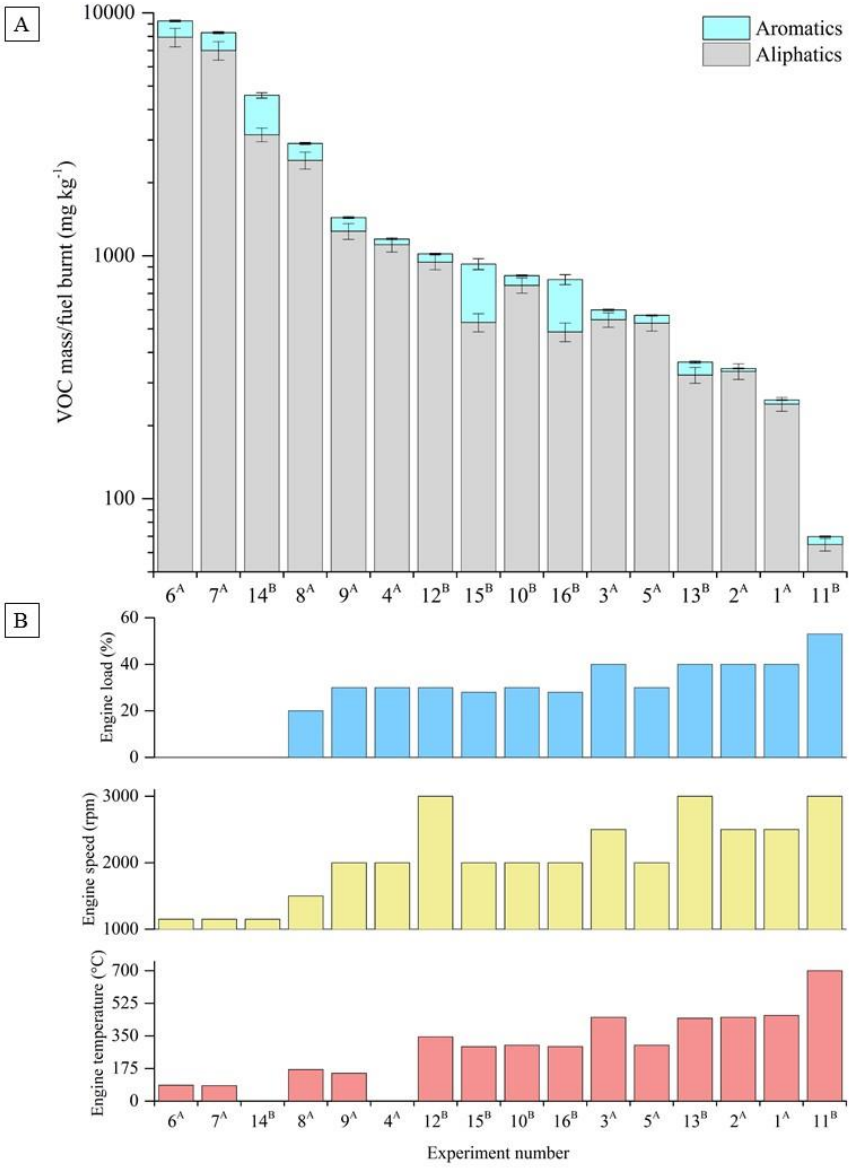

Figure 6 –Total speciated VOC-IVOC emission rate (∑SpVOC) measured in each experiment (refer to Table 1) divided into aliphatic and aromatic emissions rates (A). Experiments ordered from left-to-right by decreasing VOC-IVOC emission rates. Engine temperature, speed and load in each corresponding experiment is shown in (B). ^{A} = Fuel batch A used (see sections 2.2 and 3.1.1). ^{B} = Fuel batch B used. No DOC in exp. 3. Sequence of engine conditions performed in exp. 9 and 8 (see section 2.3 and SI Figure S2). No engine temperature measurement for exp. 4 and 14 (engine thermocouple unresponsive). Error bars represent the calculated uncertainty in the measured emission rates, see the SI section 1.1 for further information.